Biochemistry

 Volume 34, Number 20 May 23, 1995

Accelerated Publications

Site-Specific Cross-Linking as a Method for Studying Intramolecular Electron Transfer†

Helen S. Pappa and Thomas L. Poulos*

Departments of Molecular Biology and Biochemistry and Physiology and Biophysics, University of California, Irvine, Irvine, California 92717

Received March 13, 1995; Revised Manuscript Received April 6, 1995®

ABSTRACT: Site-directed mutagenesis has been used to introduce cysteine residues into yeast cytochrome *c* peroxidase and yeast cytochrome *c* for the purpose of forming site-specific cross-linked intermolecular complexes. This enables the formation of well-defined homogeneous covalently linked complexes for the purpose of relating structure to intramolecular electron transfer. Two complexes have been prepared and analyzed. Complex **I** has an engineered cysteine at position 290 near the C-terminus of the peroxidase linked to the naturally occurring Cys102 near the C-terminus of yeast cytochrome *c*. This complex exhibits undetectable rates of intramolecular electron transfer. Complex **II** has Cys290 of the peroxidase linked to the engineered Cys73 of cyt *c*. This complex was designed to mimic the crystal structure of the peroxidase−cytochrome *c* noncovalent complex [Pelletier & Kraut (1992) *Science 258*, 1748−1755]. Stopped-flow studies show that complex **II** carries out intramolecular electron transfer from ferrocytochrome *c* to peroxidase compound **I** at a rate of ≈500−800 s^{-1}. This indicates that the binding orientation observed in the crystal structure is competent in rapid intramolecular electron transfer.

Many biological electron-transfer reactions require the formation of protein−protein complexes where the distance between redox centers is large, >10 Å. Much current work focuses on attempting to define the various parameters defined by Marcus theory (Marcus & Sutin, 1985) that control electron-transfer rates such as the donor-to-acceptor distance, reorganization energy, thermodynamic driving force ($\Delta G°$), intervening medium, and donor−acceptor orientation. Two distinct views have emerged on the role the protein plays in controlling these parameters. In the first view, the intervening medium between redox centers is considered to play a critical role in the electron-transfer process (Karpishin *et al.*, 1994). In this case, redox proteins are "wired" with selective electron-transfer routes from donor to acceptor. In the second, the protein medium is viewed as a "passive" carrier of redox centers, and the rate of electron transfer is controlled primarily by the donor−acceptor distance (Moser *et al.*, 1992). It may well be that electron transfer is controlled by either one or both types of mechanisms (Evenson & Karplus, 1993; Friesner, 1994).

Selective ruthenation of metalloproteins, like cytochrome c and myoglobin, has proven to be an excellent experimental system for deciphering the role that the intervening medium and distance play in electron transfer (Winkler *et al.*, 1982; Geren *et al.*, 1991). The location of the ruthenium can be strictly controlled using site-directed mutagenesis (Bowler

† This work was supported by a grant from the National Institutes of Health.

* To whom correspondence should be addressed at the Department of Physiology and Biophysics [telephone, (714) 824-7020; FAX, (714) 824-8540; e-mail, poulos@indigo3.biomol.uci.edu].

® Abstract published in *Advance ACS Abstracts,* May 1, 1995.

0006-2960/95/0434-6573$09.00/0

et al., 1989), thus providing a structurally well-defined system for studying the electron-transfer reaction between the ruthenium and heme iron atoms. It would be highly desirable to have similarly well-defined covalently linked protein−protein complexes where the two proteins are natural redox partners. Chemical cross-linking has been used to tether two redox partners together (Erman *et al.*, 1987; Alleyne *et al.*, 1992), thereby providing a system for studying unimolecular electron transfer and avoiding the more complex bimolecular kinetics of the noncovalent complexes. However, these approaches have met with limited success owing to heterogeneity of the covalent complexes. In addition, some of the chemically cross-linked complexes (Peerey & Kostic, 1989) do not show significant rates of intramolecular electron transfer, most likely because the two proteins were not cross-linked at their optimal orientation for efficient electron transfer.

Such problems could be avoided if one engineered well-defined sites for covalent cross-linking, such as cysteine residues, onto the surface of the two redox partners so that a 1:1 homogeneous covalent complex can be produced. To apply site-specific cross-linking to the study of protein−protein electron transfer, at least two experimental criteria must be met. First, both the donor and acceptor must be produced in recombinant systems where generating site-directed mutants is possible. Second, the crystal structure of each must be known. The cytochrome *c* peroxidase (CCP)[1] and yeast cytochrome *c* (cyt *c*) electron-transfer system satisfies both criteria.

CCP catalyzes the peroxide-dependent oxidation of cyt *c* in the following multistep reaction:

$$\mathrm{CCP(Fe^{3+}) + H_2O_2 \rightarrow \underset{\text{compound I}}{CCP(Fe^{4+}\ Trp191^{\bullet})} + H_2}$$

$$\mathrm{\underset{\text{compound I}}{CCP(Fe^{4+}\ Trp191^{\bullet})} + \text{cyt } c(Fe^{2+}) \rightarrow CCP(Fe^{4+}\ Trp191) + \text{cyt } c(Fe^{3+})}$$

$$\mathrm{CCP(Fe^{4+}\ Trp191) + \text{cyt } c(Fe^{2+}) \rightarrow CCP(Fe^{3+}\ Trp191) + \text{cyt } c(Fe^{3+})}$$

This system has been extensively studied, and recently the crystal structure of the noncovalent complex was determined (Pelletier & Kraut, 1992). This structure leads to a proposed electron-transfer path involving Trp191, a residue thought to be the site of free radical formation in compound **I** (Sivaraja *et al.*, 1989) and also known to be essential for activity (Mauro *et al.*, 1988). This, however, may represent only one possibility. CCP has two sites for cyt *c* binding, one weak and one strong (Stemp & Hoffman, 1993; Zhou & Hoffman, 1994). Zhou and Hoffman (1994) suggest that the Pelletier and Kraut crystal structure of the noncovalent complex is the high-affinity site with a low electron-transfer rate while the second site proposed by Northrup *et al.* (1988) is the weak-affinity, fast electron-transfer rate site. In order to decipher which are active interaction domains, we have developed a site-specific cross-linking method to covalently tether cyt *c* to CCP at precisely defined sites and follow intramolecular electron transfer using stopped-flow methods. Two complexes have been prepared in which S−S bridges are used to covalently link the two proteins. The tail-to-tail complex has an S−S bridge between the naturally occurring Cys102 near the C-terminus of yeast iso-1-cyt *c* and an engineered Cys near the C-terminus of CCP at position 290. The second complex was designed to mimic the Pelletier−Kraut model, and in this complex, an S−S bridge is formed between the engineered Cys residues at positions 290 in CCP and 73 in cyt *c*.

MATERIALS AND METHODS

Materials. Baker's yeast cyt *c* was kindly donated by Dr. T Yonetani (University of Pennsylvania), and horse heart cyt *c* (type VI) was purchased from Sigma Chemical Co. All other common chemicals used were the highest grade and were also purchased from Sigma Chemical Co.

Mutagenesis. Mutants of CCP were constructed in the *Escherichia coli* expression plasmid PT-7 (Darwish *et al.*, 1991) using the method of Kunkel *et al.* (1987) as previously described (Choudhury *et al.*, 1994). The oligonucleotides used for constructing the Cys128 → Ala128 and the Glu290 → Cys290 mutants are 5′-CCA TGG AGA **GCT** GGT AGA GTC GAC-3′ and 5′-AAG ACT TTA **TGT** GAA CAA GGT TTA-3′, respectively.

The yeast cyt *c* mutagenesis was carried out with pBUG vector (a gift from Dr. G. Pielak, University of North Carolina). The naturally occurring Cys102 in yeast iso-1-cyt *c* has been converted to Thr, and this mutant is designated wild-type cyt *c* (Cutler *et al.*, 1987). The Lys73 → Cys73 mutation was introduced using the method of Kunkel *et al.* (1987). A 27-base oligonucleotide primer with the sequence 5′-ACC AGG AAT ATA **GCA** CTT TGG GTT AGT-3′ was used to convert the AAA (Lys) codon to TGC (Cys).

Protein Purification. Wild-type and mutant CCP were purified as previously described (Fishel *et al.*, 1987; Choudhury *et al.*, 1994). The proteins were twice crystallized by dialysis against cold distilled water, and the CCP concentration was estimated spectrophotometrically using an extinction coefficient at 408 nm of 96 m M^{-1} cm^{-1}.

The (C73T102) cyt *c* variant was expressed in the *Saccharomyces cerevisiae* cell line B-6748 (MATa cyc1-D::lacZ cyc7-D::CYH2 ura3-52 his3-D1 leu2-3 leu2-112 trp1-289 can1-100 cyh2) (Holzchu *et al.*, 1987). The B-6748 cell line has been engineered not to express either iso-1-cyt *c* or iso-2-cyt *c* owing to chromosomal insertions/deletions (Holzchu *et al.*, 1987). Cyt *c* from 9.0 L of cell culture was purified as described (Cutler *et al.*, 1987) with the exception of the last chromatographic step as follows. Cyt *c* in 50 mM cacodylate buffer, pH 6.5, was loaded on a 15-mL CM32 column equilibrated with the same buffer. The column was thoroughly washed with 50 mM cacodylate buffer, pH 6.5, followed by 100 mM KP_i, pH 6.5. The cyt *c* eluted from the column only after a 200 mM KP_i, pH 7.8, buffer was applied. In most cases, the cyt *c* was 99% pure after the CM32 column as judged by SDS−PAGE. However, if any contaminants were detected, the protein was finally purified through a long S-100 gel filtration column. The cyt *c* concentration was estimated spectrophotometrically at 410 nm using an extinction coefficient of 106 mM^{-1} cm^{-1}.

[1] Abbreviations: CCP, cytochrome *c* peroxidase; CCPI, cytochrome *c* peroxidase compound I; R_{sym}, the scaling residual between symmetry-related reflections given by $R_{sym} = \sum|I_i - \langle I_i\rangle|/\sum I_i$, where I_i = intensity of *i*th observation and $\langle I_i\rangle$ = mean intensity; *R*-factor, $\sum|F_o - F_c|/\sum F_o$, where F_c = calculated and F_o = observed structure factors.

Determination of the Cyt c Redox Potentials. The redox potentials of the different cytochromes were measured by square wave voltammetry (Osteryoung, 1991). The reference electrode was a saturated calomel with a potential of 240 mV versus the normal hydrogen electrode. The potentials used were from −200 mV to 400 mV with a step of 3.7 mV and 25 Hz frequency. The measuring electrode was polished with alumina and coated with a saturated solution of aldrithiol-4. All measurements were performed in 50 mM KP_i and 0.1 M KCl, pH 7.0. The protein concentrations were 0.12 mM for horse cyt *c*, 0.11 mM for (K73C102) yeast cyt *c* and 0.10 mM for (C73T102) yeast cyt *c*.

X-ray Diffraction Studies of (A128)CCP. Diffraction quality crystals were obtained for the Ala128 mutant from 2-methyl-2,4-pentanediol (MPD) as described by Edwards and Poulos (1991) and Sundaramoorthy *et al.* (1993). Using a Siemens area detector and rotating anode x-ray source, a total of 166 478 observations of 17 758 unique reflections to 2.3 Å were collected from a single crystal and scaled to give an $R_{sym} = 0.072$. The data were complete to 2.5 Å and 60% complete in the 2.5−2.3 Å shell. The signal-to-noise ratio ($I/\sigma I$) at the highest resolution was 1.7.

Attempts to obtain diffraction quality crystals of the Glu290 → Cys290 mutant were not successful. This could be due to states of Cys oxidation, the presence of thiol-protective reducing agents in crystallization trials, or the fact that position 290 is near crystalline contacts.

Cross-Linking. A 2−4-fold molar excess of each cyt *c* to CCP was used. The cross-linking conditions were the same for both wild-type and the Cys73 mutant cyt *c* and resulted in the same yields of the covalent 1:1 CCP−cyt *c* complex. The reaction mixture consisted of 0.3 mL of 0.29 mM CCP solution in 100 mM KP_i, pH 6.0, mixed with 0.5 mL of 0.45 mM yeast cyt *c* in 100 mM KP_i, pH 6.0. Cupric sulfite was added to a final concentration of 1 mM to catalyze the disulfide bond formation, and the reaction was left to proceed for 1 h on ice. The yields of cross-linked complex were the same when the reaction was proceeded at pH 6.0 and pH 7.0 and were typically 25−40% of the total protein.

The covalent complex was purified from the CCP and cyt *c* monomers and homodimers by the following procedure. The reaction mix was dialyzed against 50 mM cacodylate buffer, pH 6.5, to remove any phosphates and loaded on a 15-mL CM32 column preequilibrated with the same buffer. Washing with the same buffer eluted CCP monomers and homodimers. The CCP−cyt *c* covalent complex eluted after the column was washed with 100 mM KP_i, pH 6.0, while the cyt *c* monomers and homodimers did not elute until the column was washed with 200 mM KP_i, pH 7.8. The advantage of this purification method is that not only is it a simple one-step procedure but we can successfully isolate the non-cross-linked CCP and cyt *c* for future cross-linking experiments. In Figure 1 is shown the SDS−PAGE of the covalent complex formed between Cys290 in CCP and Cys73 in cyt *c* before and after reduction of the S−S bridge.

Steady-State Activity Assays. The activities of the CCP variants as well as the covalent complex **I** and complex **II** were determined at 20 °C according to the procedure of Fishel *et al.* (1987). The steady-state kinetic parameters were determined in 1 mL of 20 mM KP_i, pH 6.0, containing 20−40 μM yeast ferrocyt *c* and 2.7−87 μM H_2O_2. The protein concentrations were typically 0.3−0.5 nM for the wild-type CCP and CCP mutants and 4−6.5 nM for the

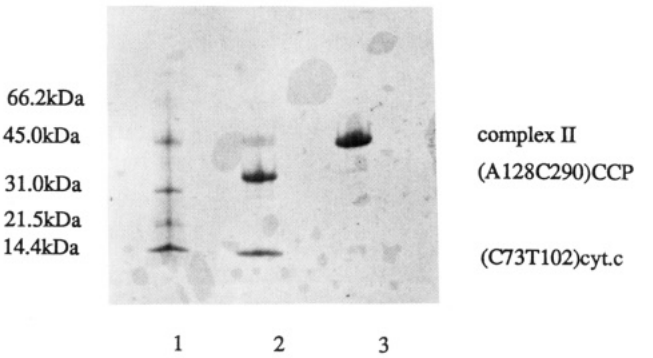

FIGURE 1: 10−15% SDS-polyacrylamide gel of the CCP−yeast cyt *c* complex covalently linked by an S−S bond between Cys290 in CCP and Cys73 in cyt *c*. Lane 1 shows molecular weight markers; lane 2 shows the complex with reducing agent; lane 3 shows the complex without reducing agent.

covalent complexes **I** and **II**. Comparisons between CCP and the cross-linked complexes were estimated from k_{cat} values taken at single concentrations of substrate.

Stopped-Flow Kinetics. Transient kinetic studies were performed on a Hi-Tech SF-51 stopped-flow spectrophotometer using 1-cm path-length cell. The output was interfaced to a Hi-Tech spectrophotometer unit SU-40 and a Compaq PC for kinetic analysis.

For estimating the rate of reduction of free cyt *c* by ascorbate, a 4.5 μM cyt *c* solution and varying concentrations of ascorbate (0.45−18 mM) were placed in 2.5-mL syringes. The reduction of cyt *c* was followed at 416 nm. The rate of reduction of the covalently attached cyt *c* in complex **II** (face-to-face complex) by ascorbate was very slow and therefore could be measured with a conventional spectrophotometer. All rates were determined in 200 mM KP_i, pH 6.0.

The rate of compound **I** formation of the CCP molecule within the covalent complex **II** was also estimated by stopped-flow spectroscopy. A 4 μM complex solution and varying concentrations of H_2O_2 (4−16 μM) were placed into the stopped-flow syringes. The compound **I** formation was measured at 425 nm.

For determining the intramolecular rate of electron transfer in the covalent complexes, the following procedure was used. The cyt *c* in the complex was reduced with ascorbate, which has no effect on CCP, and excess ascorbate removed by anaerobic gel filtration. In one syringe was the covalent complex with the cyt *c* reduced and in the second syringe a 5-fold excess of hydrogen peroxide. The peroxide oxidizes CCP to compound **I** (CCPI) followed by oxidation of cyt *c* as an electron transfers from the reduced cyt *c* to CCPI. Oxidation of cyt *c* was followed at 414 nm, an isosbestic point for CCP and CCPI. The instrumental signal-to-noise ratio limited the minimum concentration of either reactant to 2.5 μM.

For determining the dependence of the electron-transfer rate on the H_2O_2 concentration, a 2.6 μM complex solution was placed in one syringe and 5−20 μM H_2O_2 in the other, and the rate of oxidation of ferro-yeast cyt *c* was monitored at 414 nm. However, we were limited to a few H_2O_2 concentrations because the reaction was too fast to be resolved within the stopped-flow window at H_2O_2 concentrations higher than 20 μM.

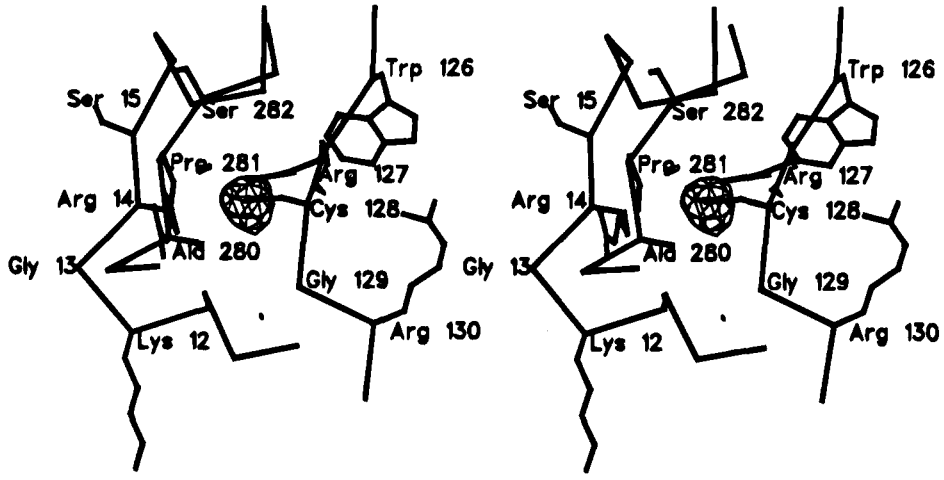

FIGURE 2: Stereoscopic diagram of the 2.3 Å $F_o - F_c$ electron density map of the (A128)CCP mutant contoured at $\pm 3\sigma$, where σ is the root-mean-square electron density computed over an entire asymmetric unit. At this level only negative contours are present. Note the large lobe of negative electron density surrounding the side chain of residue 128 which is Cys in the wild-type enzyme.

RESULTS

Characterization of the (A128)CCP Mutant. CCP contains a single cysteine at position 128. The cysteine at position 128 was replaced by alanine, and the mutant was designated (A128)CCP. The mutant CCP exhibited spectral properties in both the resting and compound **I** states indistinguishable from wild-type CCP. The steady-state activity also was the same with $k_{cat} = 400 \pm 10\ s^{-1}$ compared to $410 \pm 10\ s^{-1}$ for wild-type CCP.

The initial $F_o - F_c$ electron density difference map at 2.3 Å (Figure 2) clearly showed the missing sulfur atom. The structure was refined with X-PLOR (Brunger, 1992) to an *R*-factor = 0.20 for data between 10 and 2.3 Å. Other than the missing sulfur atom, the mutant and wild-type structures are, within experimental error, identical.

Characterization of the (A128C290)CCP Double Mutant. After eliminating the cysteine at position 128, a cysteine residue was introduced at position 290, and the double mutant was designated as (A128C290)CCP. The double mutant incorporated heme, and its UV/visible absorption spectra were very similar to wild-type CCP. However, the activity of the (A128C290)CCP toward horse ferrocyt *c* was 60–70% of the wild-type CCP activity in steady-state assays. The CCP–horse heart cyt *c* association could well be affected by the Glu290 → Cys290 substitution because it has been proposed that Glu290 of CCP forms a salt bridge with the Lys73 of the horse heart cyt *c* in the recently published structure of the noncovalent complex (Pelletier & Kraut, 1992). When the sulfhydryl group of the Cys290 was derivatized with iodoacetic acid, the double mutant regained 100% wild-type activity (data not shown). This result supports a role for a carboxyl group at position 290 in forming the complex since derivatizing Cys290 with iodoacetic acid restores the missing carboxylate.

Characterization of the (C73T102)Yeast Cyt c Mutant. Approximately 5 mg per 3 L of culture of the (C73T102) mutant could be prepared from the recombinant yeast expression system kindly provided to us by Dr. Gary Pielak. The (C73T102)yeast cyt *c* variant had the tendency to dimerize at high protein concentrations, and therefore DTT was included before any experimentation and the excess DTT removed by anaerobic gel filtration.

To confirm that the Lys73 → Cys73 substitution had no effect on the heme environment, the redox potential of the mutant was measured using square wave voltametry (Osteryoung, 1991). The redox potential was found to be 223 mV, which is in good agreement with the value of 234 mV for wild-type (K73T102) cyt *c* measured in our laboratory.

Modeling the Cross-Linked Complexes. A hypothetical model of the two covalent complexes used in this study is shown in Figure 3. Complex **I**, the tail-to-tail complex, was designed as a "negative" control. The heme edges in this complex are expected to be >30 Å apart with few nonbonded contacts to help selectively orient the complex. Complex **II** (Figure 3) was designed to mimic the Pelletier–Kraut crystal structure where the heme edges are closer to 20 Å apart and there are extensive intermolecular nonbonded contacts. In the remainder of this paper we will refer to these two complexes as complex **I** (tail-to-tail) and complex **II** (face-to-face). In the crystal structure, Lys73 of cyt *c* is close to Glu290 of CCP. Modeling studies indicated that converting each to a Cys residue would allow an S–S bridge to form if the cyt *c* rotated slightly. As shown in Figure 3, the motion required does not grossly affect the interface region between the CCP and cyt *c* hemes from that found in the crystal structure. Hence, a majority of the intermolecular contacts observed in the crystal structure and the heme–heme distance should not be significantly altered by tethering the two proteins with the S–S bridge.

Compound I Formation in the Covalent Complex. Previous covalent complexes formed by chemically cross-linking CCP to horse cyt *c* using carbodiimides did not completely form compound **I** (Erman *et al.*, 1987). These authors found that only 70% of the complex reacted successfully with hydrogen peroxide to form compound **I** while the remaining CCP existed in a form that did not react with hydrogen peroxide. This is not the case in our system. Addition of equimolar amounts of hydrogen peroxide converted all the CCP of the complex to compound **I** as estimated by the change of the extinction coefficient at 424 nm ($\Delta\epsilon_{424nm}$ = 41m $M^{-1}\ cm^{-1}$), which is in excellent agreement with the published value for wild-type CCP compound **I** formation ($\Delta\epsilon_{424nm} = 41.6\ mM^{-1}\ cm^{-1}$; Yonetani, 1965). The rate of compound **I** formation for the covalent complex **II** estimated from stopped-flow experiments is $4 \times 10^7\ M^{-1}\ s^{-1}$, which

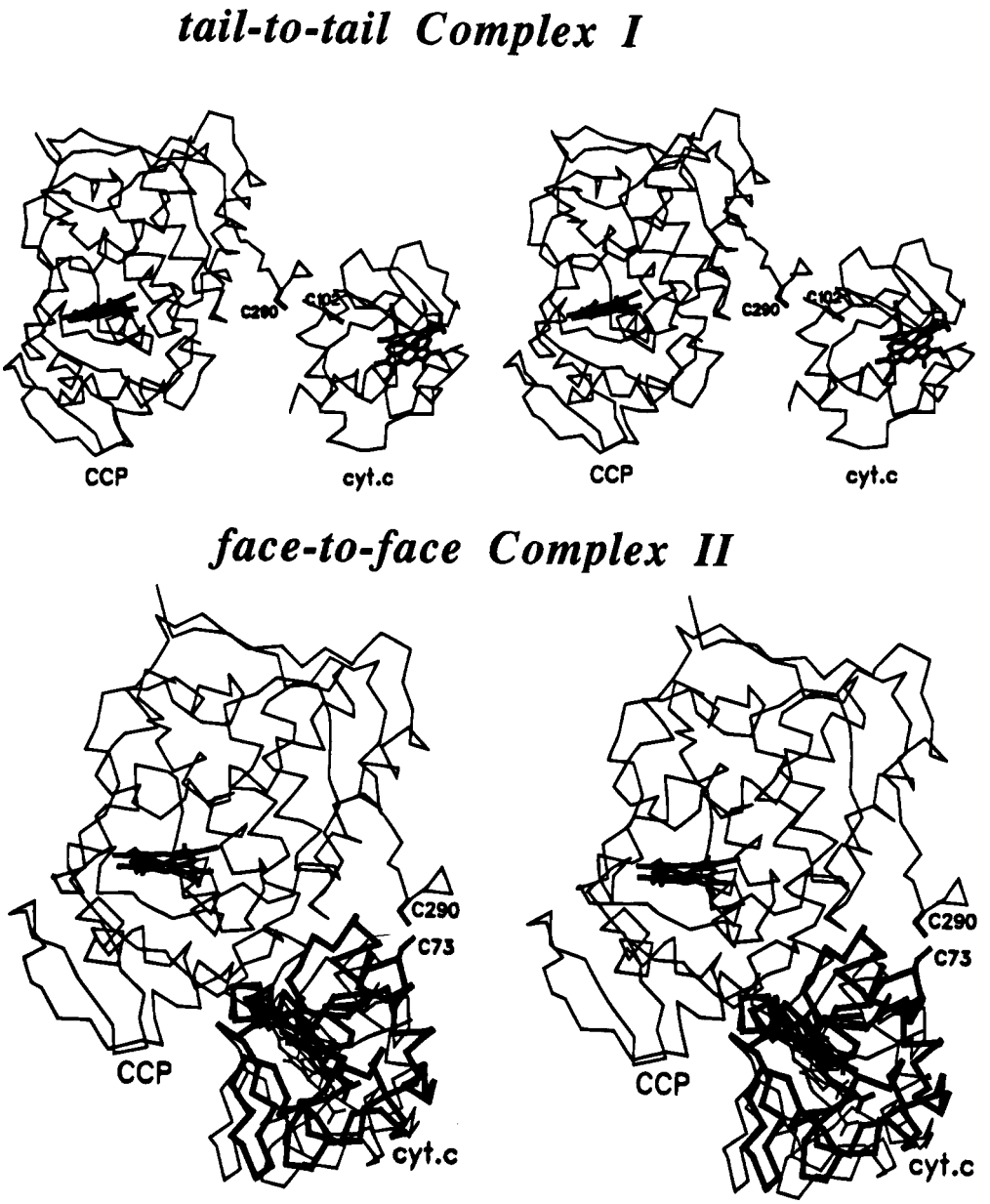

FIGURE 3: Hypothetical stereo representations of the two CCP−yeast cyt *c* covalent complexes. In the tail-to-tail complex (complex **I**), the two redox partners are cross-linked through the naturally occurring Cys102 of cyt *c* and the engineered Cys290 of CCP. In the face-to-face complex (complex **II**), the two proteins are tethered together through the Cys290 engineered in CCP and the Cys73 engineered in yeast cyt *c*. For complex **II**, the CCP−cyt *c* orientation based on the crystal structure of the complex (Pelletier & Kraut, 1992) has the cyt *c* drawn in thin lines while the modeled position of cyt *c* required to form the S−S bond is in thick lines.

is, within experimental error, identical to the rate of formation of compound **I** for native CCP, demonstrating that the covalent attachment of cyt *c* has no effect on the peroxide reaction. This is to be expected if this covalent complex mimics the Pelletier−Kraut model (1992) since in their structure, the access channel thought to be the primary route that peroxide takes in entering the CCP active site remains open.

Rate of Cyt c Reduction. The rate of cyt *c* reduction is a sensitive measure of the accessibility of the cyt *c* heme edge (Erman *et al.*, 1987). If the heme edge is buried in complex **II**, as it should be, then the rate of ascorbate reduction of cyt *c* ought to be much lower in the covalent complex than in free cyt *c*. The rate of cyt *c* reduction was measured in either the stopped flow for free cyt *c* or a conventional spectrorophotometer for complex **II**. A plot of the pseudo-first-order rate vs ascorbate concentration was linear in both cases, allowing for an estimate of the second-order rate constant. This value was 4 M^{-1} s^{-1} for free yeast cyt *c*, 5 M^{-1} s^{-1} for complex **I**, and 0.17 M^{-1} s^{-1} for complex **II**. Hence, the rate of cyt *c* reduction in complex **II** is about 24-fold slower, demonstrating that there is significant shielding of the cyt *c* heme edge in complex **II** while the heme edge in complex **I** is accessible, as expected (see Figure 3). We considered the possibility that a large excess of ascorbate might be reducing the disulfide bond. However, the complex remained intact after being boiled in SDS buffer containing a large excess of ascorbate.

Steady-State Kinetics. The ability of both covalent complexes to oxidize exogenous cyt *c* was assayed using the conventional steady-state assay outlined in Materials and Methods. Complex **II** exhibited only 2.2% and 9.7% wild-

type levels of activity toward horse heart cyt *c* and yeast cyt *c*, respectively. The covalent tail-to-tail complex **I** was 5% and 35% active toward horse and yeast cyt *c*, respectively. These results suggest that one of the primary cyt *c* interaction sites with CCP has been blocked by the covalently attached cyt *c* molecule. On the other hand, the higher activities observed for the yeast ferrocyt *c* reaction indicate that there are other favorable interaction sites between CCP and yeast cyt *c*. The very low activities obtained for the horse heart cyt *c* indicate that the region masked by the covalently attached cyt *c* in Complex **II** is the major interaction site of CCP with horse heart cyt c.

Stopped-Flow Spectroscopy for Determining the Intramolecular Electron-Transfer Rate of the Covalent Complexes. The intramolecular electron transfer between CCP compound **I** and cyt *c* in the covalent complex was studied using the stopped-flow protocol described in Materials and Methods. Mixing 2.5 μM complex **II** with 12 μM H_2O_2 resulted in a transient (Figure 4) with a rate constant of 228 $\pm$ 20 s^{-1} and an absorbance change which corresponds to $\approx$20% of the theoretical value expected for complete oxidation of ferrocyt *c*. Therefore, a substantial portion of the reaction was too fast to be resolved in the stopped-flow spectrophotometer. The amount of cyt *c* oxidized within the dead time of the instrument increased as k_{obs} increased, and eventually there was an insufficient signal to measure k_{obs}. At the completion of the reaction, all the cyt *c* had been oxidzed. The rate of oxidation of the cyt *c* within the complex was dependent upon the hydrogen peroxide concentration (inset, Figure 4B). Within experimental error, the rate of oxidation of the covalently bound ferrocyt *c* is identical with the rate of oxidation of CCP by hydrogen peroxide. This indicates that the reaction between the complex and hydrogen peroxide, k_1 in the scheme shown below, is rate-limiting and that electron transfer between covalently bound ferrocyt *c* and CCP, k_2, is significantly faster.

$$\text{CCP}-\text{cyt } c(\text{Fe}^{2+}) \xrightarrow{k_1}$$

$$\text{CCP compound I}-\text{cyt } c(\text{Fe}^{2+}) \xrightarrow{k_2}$$

$$\text{CCP compound II}-\text{cyt } c(\text{Fe}^{3+})$$

In theory, by increasing the hydrogen peroxide concentration, we can increase $k_1[H_2O_2]$ until it is larger than k_2. In practice, the mixing time of our stopped-flow apparatus limits the maximum rate that can be observed. At concentrations above 20 μM the amplitude of the reaction is too small to be measured accurately. However, these data can be used to determine a minimum value for k_2. It is quite possible that there are multiple processes involved within the $\approx$2–3 ms dead time including an extremely fast electron transfer from cyt *c* to the Trp191 radical as found by Geren *et al.* (1991). However, if we assume the simplest case where $\approx$80% of the reaction that is complete within $\approx$2–3 ms (Figure 4B) follows a single first-order process, we can estimate k_2 as follows:

$$(\text{cyt } c \text{ at time} = 0)/(\text{cyt } c \text{ at time } t) =$$

$$\exp(k_2\Delta t) \text{ or } 1/0.2 = \exp(k_2 \times 2 \text{ or } 3) \text{ and}$$

$$k_2 = 500-800 \text{ s}^{-1}$$

Although there is a large error in estimating k_2 owing to the lack of precision in determining the instrument dead time

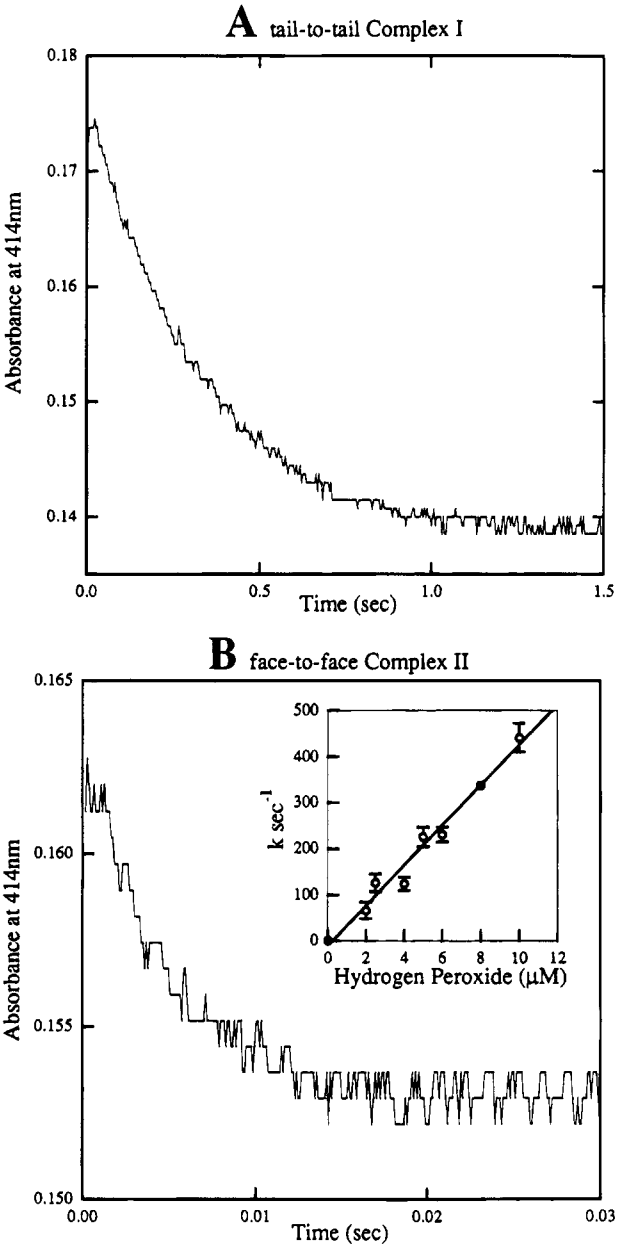

FIGURE 4: Stopped-flow traces showing the rate of ferrocyt *c* oxidation by CCP compound I followed at 414 nm: (A) 2.5 μM complex **I** (tail-to-tail) mixed with 12 μM H_2O_2. (B) 2.5 μM complex **II** (face-to-face) mixed with 12 μM H_2O_2. The inset in B shows the dependence of the pseudo-first-order rate on peroxide concentration.

and the simple first-order assumption, 500–800 s^{-1} falls within the 350–1500 s^{-1} range found using both stopped-flow (Hahm *et al.*, 1994; Summers & Erman, 1988) and laser flash techniques (Hazzard *et al.*, 1988a,b; Geren *et al.*, 1991) for both the covalent (Erman *et al.*, 1987; Hazzard *et al.*, 1988) and noncovalent complexes (Summers & Erman, 1988; Hazzard *et al.*, 1987) although there is some inconsistency in the literature since Geren et al. (1991) estimate a rate of cyt *c* oxidation $\approx$50 000 s^{-1}. These data indicate that the covalent complex **II** carries out intramolecular electron transfer at least as fast as that estimated from several other studies. The electron-transfer rates observed for the tail-to-tail complex **I** were very different than those of the face-to-face complex **II**. The oxidation of cytochrome *c* shown in Figure 4A was much slower, $\approx$1.5 s^{-1}, and gave an absorbance change which corresponds to the theoretical value

expected for complete oxidation of ferrocyt *c*. The rate of electron transfer was independent of H_2O_2 concentration as expected since $k_1[H_2O_2] \gg k_2$, but it was directly dependent on the complex concentration, indicating that the electron-transfer event observed is intermolecular rather than intramolecular. Therefore, if intramolecular electron transfer occurs at all, the rate is orders of magnitude slower than was observed in complex **II**. These results were expected because the CCP and cyt *c* within complex **I** are oriented in such a way that the heme of cyt *c* is available to react with CCP from another complex **I** molecule (Figure 3).

DISCUSSION

The CCP−cyt *c* system has been a paradigm for interprotein electron-transfer reactions for a number of years. This was one of the first systems to be used for covalently linking two proteins together in an attempt to trap a redox complex in an active orientation (Bisson & Capaldi,1981; Waldmeyer *et al.*, 1980). The results have been encouraging since the complexes exhibit intramolecular electron-transfer rates comparable to that found in the noncovalent complex (Hazzard *et al.*, 1988a,b; Geren *et al.*, 1991). Nevertheless, it has proven difficult to structurally characterize these complexes owing to the nonspecific cross-linking agents used and the heterogeneity of the resulting covalent complexes. Other systems give very different results since the covalently linked complexes exhibit very low levels of activity (Peery & Kostic, 1989; Walker *et al.*, 1990; Alleyne *et al.*, 1992). These complexes generally are formed at low ionic strength which may select for the electrostatically most stable complex but not the most active complex.

Our goal in this work was to extend the cross-linking approach with CCP by using site-directed mutagenesis to prepare precisely defined cross-linking sites that will generate homogeneous complexes and allow for a more penetrating probe on the relationship between structure and the various parameters that control intramolecular electron transfer. Very recently, Wang and Margoliash (1995) have taken a step in this direction by attaching a photoactive group to engineered cysteine residues in cytochrome *c* and then cross-linked the site specifically modified cytochrome *c* to CCP. There still is the uncertainty of where on CCP the cross-link occurs. The next obvious step, which we have taken, is to engineer both CCP and cytochrome *c* so we know precisely which two residues are cross-linked. In many respects this approach is similar to the ruthenated procedures where the ruthenium is moved to any desired location on the surface of a metalloprotein (Winkler & Gray, 1992). In our case, we move an entire protein.

In choosing where to place the Cys residues, we used the crystal structure of the noncovalent complex formed between CCP and cyt *c* (Pelletier & Kraut, 1992) as a guide. The structures of both the CCP−yeast cyt *c* and CCP−horse heart cyt *c* noncovalent complexes show that Lys73 of cyt *c* is close to Glu290 of CCP. Formation of an S−S bridge has strict stereochemical restraints, and these restraints were built into the model shown in Figure 3. Even with these restrictions, the interface between CCP and cyt *c* near the cyt *c* heme edge should not be grossly perturbed relative to the crystal structure. Thus, the formation of this S−S bridge should form a complex that closely resembles the Pelletier and Kraut structures (1992) and allow for a direct experimental test on whether this complex is competent in intramolecular electron transfer. We also cross-linked the CCP Ala128/Cys290 mutant to the naturally occurring Cys102 in yeast iso-1-cyt *c* for two reasons: first, to see if a cross-link could be formed in reasonable yields between regions of the proteins that are not specifically designed to recognize one another and, second, to see if simply tethering CCP to cyt *c* is sufficient to achieve good rates of electron transfer. Apparently this is not sufficient since the electron-transfer rate was on the order of 1.5 s^{-1} and appeared to be intermolecular rather than intramolecular. This means that the cyt *c* heme edge must be available to CCP from another complex **I** molecule. That the cyt *c* heme edge indeed is available is evidenced by the rate of cyt *c* reduction by ascorbate in complex **I**, which is about the same as in free cyt *c*.

In contrast, complex **II** exhibited a very fast intramolecular electron-transfer rate. About 80% of the cyt *c* is reduced within the dead time of the stopped-flow instrument, giving a lower estimate of ≈500−800 s^{-1} for the intramolecular electron-transfer rate. This estimate is based on the assumption that the entire electron-transfer reaction follows a simple first-order process with only one rate. There could well be a much faster process as indicated by the work of Geren *et al.* (1991) and Hahm *et al.* (1992). Nevertheless, the 500−800 s^{-1} rate is within the 350−1500 s^{-1} range found for both the noncovalent complex (Hazzard *et al.*, 1987; Geren *et al.*, 1991) and the nonspecifically cross-linked complexes (Erman *et al.*, 1987; Hazzard *et al.*, 1988) using both stopped-flow and laser flash techniques (Summers & Erman, 1988; Hazzard *et al.*, 1987). Most importantly, the structure of the face-to-face complex **II** is probably very nearly the same as the Pelletier and Kraut crystal structures (1992) and indicates that the orientation of CCP and cyt *c* observed in the crystal structure of the noncovalent complexes is competent in electron transfer. Two important properties of complex **II** indicate that this is the case. First, the CCP in complex **II** reacts with H_2O_2 at the same rate as free wild-type CCP to give 100% conversion to compound **I**. This indicates that the peroxide access channel remains open in complex **II**. Second, the rate of reduction of cyt *c* by ascorbate is 24-fold slower than for free cyt *c*. This shows that the cyt *c* heme is relatively inaccessible in the complex, as expected from the crystal structure. It also appears that, in complex **II**, one of the primary sites for interaction with exogenous cyt *c* has been blocked. In the steady-state assay, the rate of oxidation of yeast cyt *c* and horse heart cyt *c* by CCP in the complex is 9.7% and 2.2% of wild type, respectively. Although these represent a large drop in rates, the residual activity demonstrates that there is at least one additional site for binding of cyt *c*, as expected (Zhou & Hoffman, 1994). Interestingly, the site predicted by Northrup *et al.* (1988) centered around Asp148 in CCP remains open in complex **II**.

In summary, a combination of site-specific mutagenesis and sulfhydryl chemistry has been shown to be a useful method for preparing a well-defined and homogeneous covalently linked redox complex that exhibits a physiologically relevant rate of intramolecular electron transfer. The properties of the face-to-face complex **II** closely match those predicted from the crystal structure of the noncovalent complex. These results support the proposal by Pelletier and Kraut that the orientation of CCP and cyt *c* observed in the

crystal structure exhibits physiologically relevant intramolecular electron-transfer rates.

ACKNOWLEDGMENT

We thank Dr. M. Sundaramoorthy for his guidance in solving the crystal structure of the (A128)CCP. We also thank Drs. Gary Pielak and Aleister Saunders (University of North Carolina) for invaluable advice and materials needed for the expression of yeast cyt *c*, Prof. A. E. G. Cass (Imperial College, London, U.K.) for performing the redox potential measurements, and Dr. Takashi Yonetani for baker's yeast cyt *c*.

REFERENCES

Alleyne, T. A., Wilson, M. T., Antonini, G., Malatesta, F., Vallone, B., Sarti, P., & Brunori, M. (1992) *Biochem. J. 287*, 951−956.
Bisson, R., & Capaldi, R. A. (1981) *J. Biol. Chem. 256*, 4362−4367.
Bowler, B. E., Meade, T. J., Mayo, S. L., Richards, J. H., & Gray, H. B. (1989) *J. Am. Chem. Soc. 111*, 8757.
Brunger, A. T. (1992) *X-PLOR Version 3.1: A System for X-Ray Crystallography and NMR*, Yale University Press, New Haven.
Choudhury, K., Sundaramoorthy, M., Hickman, A., Yonetani, T., Woehl, E., Dunn, M. F., & Poulos, T. L. (1994) *J. Biol. Chem. 269*, 20239−20249.
Darwish, K., Li, H., & Poulos, T. L. (1991) *Protein Eng. 4*, 701−708.
Edwards, S. E., & Poulos, T. L. (1990) *J. Biol. Chem. 265*, 2588−2595.
Erman, J. E., Kim, K. L., Vitello, L. B., Moench, S. J., & Saterlee, J. D. (1987) *Biochim. Biophys. Acta 911*, 1−10.
Evenson, J. W., & Karplus, M. (1993) *Science 262*, 1247−1249.
Fishel, L. A., Villafranca, J. E., Mauro, J. M., & Kraut, J. (1987) *Biochemistry 26*, 351−360.
Friesner, R. A. (1994) *Structure 2*, 339−343.
Geren, L., Hahm, S., Durham, B., & Millett, F. (1991) *Biochemistry 30*, 9450−9457.
Hahm, S., Durham, B., & Millett, F. (1992) *Biochemistry 31*, 3472−3477.
Hahm, S., Miller, M. A., Geren, L., Kraut, J., Durham, B., & Millett, F. (1994) *Biochemistry 33*, 1473−1480.
Hazzard, J. T., Poulos, T. L., & Tollin, G. (1987) *Biochemistry 26*, 2836−2848.
Hazzard, J. T., Moench, S. J., Erman, J. E., Satterlee, J. D., & Tollin, G. (1988a) *Biochemistry 27*, 2002−2008.
Hazzard, J. T., McLendon, G., Cusanovich, M. A., & Tollin, G. (1988b) *Biochem. Biophys. Res. Commun. 151*, 429−434.
Holzchu, D., Principio, L., Conklin, K. T., Hickey, D. R., Short, J., Rao, R., McLendon, G., & Sherman, F. (1987) *J. Biol. Chem. 262*, 7125−7131.
Karpishin, T. B., Grinstaff, M. W., Komar-Panicucci, S., McLendon, G., & Gray, H. (1994) *Structure 2*, 415−422.
Kunkel, T. A., Roberts, J. D., & Zokour, R. A. (1987) *Methods Enzymol. 154*, 367−382.
Marcus, R. A., & Sutin, N. (1985) *Biochim. Biophys. Acta 811*, 265−322.
Mauro, J. M., Fishel, L. A., Hazzard, J. T., Meyer, T. E., Tollin, G., Cusanovich, M. A., & Kraut, J. (1988) *Biochemistry 27*, 6243−6256.
Moser, C. C., Keske, J. M., Warncke, K., Farid, R. S., & Dutton, P. L. (1992) *Nature 355*, 796−802.
Northrup, S. H., Boles, J. O., & Reynolds, J. C. L. (1988) *Science 241*, 67−70.
Osteryoung, J. (1991) *Anal. Chem. Res. 63*, 2743−2750.
Peery, L. M., & Kostic, N. M. (1989) *Biochemistry 28*, 1861−1868.
Pelletier, H., & Kraut, J. (1992) *Science 258*, 1748−1755.
Sivaraja, M., Goodin, D. B., Smith, M., & Hoffman, B. M. (1989) *Science 245*, 738−740.
Stemp, E. D. A., & Hoffman, B. M. (1993) *Biochemistry 32*, 10848−10865.
Summers, F. E., & Erman, J. E. (1988) *J. Biol. Chem. 263*, 14267−14275.
Waldmeyer, B., Bechtold, R., Zurrer, M., & Bosshard, H. R. (1980) *FEBS Lett. 119*, 349−351.
Walker, M. C., Pueyo, J. J., Gomez-Moreno, C., & Tollin, G. (1990) *Arch. Biochem. Biophys. 281*, 76−83.
Wang, Y. & Margoliash, E. (1995) *Biochemistry 34*, 1948−1958.
Winkler, J. R., & Gray, H. B. (1992) *Chem. Rev. 92*, 369−378.
Winkler, J. R., Nocera, D. J., Yokom, K. M., Bordignon, E., & Gray, H. B. (1982) *J. Am. Chem. Soc. 104*, 5798−5800.
Yonetani, T. (1965) *J. Biol. Chem. 240*, 4509.
Zhou, J. S., & Hoffman, B. M. (1994) *Science 265*, 1693−1696.

BI9505528